Radio-Opaque and Surface-Functionalized Polymer Microparticles: Potentially Safer Biomaterials for Different Injection Therapies

Ketie Saralidze,[†] Menno L. W. Knetsch,[†,‡] Catharina S. J. van Hooy-Corstjens,[†] and Leo H. Koole*[,†,‡]

Contribution from the Center for Biomaterials Research, University of Maastricht, PO Box 616, 6200 MD Maastricht, The Netherlands, and Faculty of Biomedical Engineering, Eindhoven University of Technology, Eindhoven, The Netherlands

Received April 21, 2006; Revised Manuscript Received July 17, 2006

Injectable polymer particles with a diameter in the range of 30−300 μm find applications as a biomaterial in different clinical fields, such as cosmetic surgery, reconstructive surgery, and urology. However, clinical effects tend to disappear after several months, either due to migration of the particles away from the injection site (caused by weak adherence with the surrounding soft tissues) or due to fibrosis (caused by excessive encapsulation of the particles by fibrous tissue). Little is known about the fate of injected microparticles, due to the fact that they are extremely difficult to trace in a noninvasive manner. Design, synthesis, and characterization of new polymeric microspheres with two additional features that can enhance safety and can help to overcome drawbacks of existing products are reported. First, the new microparticles feature clear radio-opacity (X-ray visibility) as they are prepared on the basis of a reactive methacrylic monomer that contains covalently bound iodine. Model experiments reveal that the level of X-ray contrast is sufficient for clinical monitoring; they can be visualized both during the injection and afterward. The particles feature excellent cytocompatibility in vitro and in vivo. Second, a method is explored to functionalize the surface of the particles, for example, through immobilization of collagen. Other extracellular matrix proteins can also be immobilized, and this provides a mechanism to control anchoring of the particles in soft tissue. The results are briefly discussed in the context of improved biomaterials, contemporary X-ray imaging, and control over biomaterial−soft tissue interactions in vivo.

Introduction

Several medical treatments are based on local injection of polymeric particles with a diameter in the 30−300 μm range. Augmentation of soft tissues (e.g., correction of lips[1] and reduction of wrinkles,[2]) can be achieved through local injection of a "filler agent", which is a suspension of nondegradable synthetic microparticles in a biodegradable solution or dispersion.[3] Another example is found in urology: stress urinary incontinence in women (SUI), defined as the complaints of involuntary leakage of urine on effort or exercise, sneezing or coughing, can be treated through precise peri-urethral injection of polymeric particles.[4]

There are concerns, however, about possible complications and long-term effects of injected polymeric microspheres.[5] Cosmetic fillers can induce the formation of granulomatous tissue, or they may migrate away from the site of injection.[6] Zullo et al. have reported that peri-urethral injection of poly(dimethylsiloxane) (PDMS) particles to treat SUI had a high initial success rate (90% after 1 month), which decreased to 75% after 3 months and 57% after 60 months.[7] This pattern was confirmed in a series of other publications.[8] These disappointing long-term effects have been attributed, quite generally, to the migratory aptitude of injected microparticles. Indeed, poly(tetrafluoroethylene) (PTFE) particles can migrate from the injection site into lungs and brain.[9] Analogously, carbon-coated ZrO_2 microbeads (Durasphere),[10] injected to treat SUI in patients, were found to migrate into local and distant lymph nodes, and into urethral mucosa.[11] The marginal long-term results have prompted the industry to introduce a variety of new bulking agents, especially with respect to SUI treatment. Most of these agents actually consist of a classic inert biomaterial with a well-established record of safety and durability, albeit in totally different applications. The most important examples, after PTFE, PDMS, and Durasphere are glutaraldehyde cross-linked bovine collagen (GAX collagen),[12] calcium hydroxyapatite,[13] dextranomer/hyaluronic acid copolymer (Dx/HA),[14] and autologous fat.[15] Claims of improved performance in SUI treatment were usually unsubstantiated. Some new agents even led to complications, such as pulmonary embolism (autologous fat)[16] or a severe local inflammatory response (GAX collagen).[17]

Migration of injected or implanted microparticles has been studied in animal models but, to the best of our knowledge, only scarcely in humans.[6a] This may be explained, in part, by the fact that commercial particles are extremely difficult to trace in vivo. The only exception is Durasphere, for which the particles have a core of ZrO_2, a notoriously radio-opaque material.[10,11] However, Durasphere particles are not particularly suitable for long-term model studies in animals; the high density of ZrO_2 (5.89×10^3 kg/m^3) may lead to movement of the particles due to gravitation. Here, we report on new polymeric microspheres that combine soft-tissue-like density with intrinsic radio-opacity; one of the building blocks is **1**, a methacrylate monomer that contains three covalently bound iodine atoms.[18]

* To whom correspondence should be addressed. E-mail: l.koole@bioch.unimaas.nl. Tel.: +31-43-3881531. Fax: +31-43-3884159.

[†] University of Maastricht.

[‡] Eindhoven University of Technology.

10.1021/bm0603903 CCC: $33.50
Published on Web 10/06/2006

The iodine-containing microparticles are stable in vivo, and they feature a high level of biocompatibility, both in vitro and in vivo. Their radio-opacity allows for accurate noninvasive monitoring through X-ray fluoroscopy and micro-CT techniques.

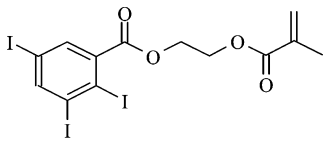

1

Furthermore, our microspheres have a reactive surface, which can be used to immobilize a plethora of compounds, such as collagen and other proteins. First, the new particles are useful vehicles to study the problem of injected-particle migration in animal models. Second, the pertaining question whether the anchoring of injected particles in soft-tissues can be improved through surface-tethering of molecules that are recognized biologically can be addressed. Ultimately, the use of radio-opaque and surface-modified polymeric microparticles as described here may open the way to safer and improved methods to treat SUI or to achieve safer and more long-lasting therapies in cosmetic surgery.

Experimental Section

Materials. Chemicals were purchased from Sigma/Aldrich/Fluka, Acros, or Invitrogen. Methyl methacrylate (MMA) was distilled at atmospheric pressure and stored at −20 °C. 2-Hydroxyethyl methacrylate (HEMA) was distilled in vacuo and stored at −20 °C. The monomer 2-[2′,3′,5′-triiodobenzoyl]-oxo-ethyl methacrylate (**1**) was prepared as described previously.[18d,f] All other commercially available chemicals were used as received. Porcine alkaline phosphatase and FITC-labeled collagen (type I, bovine) were from Sigma. Buffer solutions were prepared as follows. MES buffer: 2-(*N*-morpholino)ethanesulfonic acid (MES, 9.76 g, 50 mmol) was dissolved in 1 L of water, and the pH was set to 5.5 with NaOH. Tris buffer: tris(hydroxyl-methyl)-aminomethane (Tris, 6.06 g, 50 mmol) was dissolved in 1 L of water, and the pH was set to 9.0 with HCl. Carbonate buffer: two solutions were made $NaHCO_3$ (4.20 g, 50 mmol) in 500 mL water and Na_2CO_3 (5.27 g, 50 mmol) in 500 mL water. These were mixed in the ratio 100 mL:285 mL (Na_2CO_3:$NaHCO_3$), which gave pH = 9.6.

Microscopy. Scanning electron micrographs were recorded with a RJ Lee Personal SEM system (Goffin-Meyvis, Etten-Leur, The Netherlands). Microspheres were sprinkled onto an aluminum stub with double-faced carbon tape. Samples were sputter-coated with gold (2 min) and examined at an accelerating voltage of 20 kV. Approximately 500 microspheres were included in the analysis of size and size distribution of each batch. Light microscopy was performed on a Leica DM-IL inverted microscope, equipped with a Sony DSC-70 digital camera. Fluorescence microscopy was performed with Nikon Eclipse E800, equipped with an RS Photometrics CoolSNAP camera.

Preparation of Microspheres. A solution of poly(vinyl alcohol) (PVA, M_w = 86 000; 99−100% hydrolyzed; 1.25 g), poly(ethylene glycol) (PEG, M_w = 1000; 1.50 g), and poly(*N*-vinyl-pyrrolidinone) (PVP, M_w = 58 000; 250 mg) in 100 mL distilled water was mechanically stirred and heated to 75 °C. MMA (5.00 g, 49.93 mmol), monomer **1** (1.00 g, 1.63 mmol), benzoyl peroxide (125 mg, 0.52 mmol), and tetra-ethylene glycol dimethacrylate (TEGDMA, 340 mg, 1.03 mmol) were mixed, and this mixture was added dropwise to the stirred aqueous PVA-PEG-PVP solution.[19] After the addition, stirring at 75 °C was continued for 3 h. The microspheres precipitated immediately as stirring was stopped, and the supernatant was decanted carefully. The microspheres were allowed to cool to room temperature, and washed (water (3×), ethanol (3×), and water (3×)). The microspheres were then taken up in boiling water (1 h), decanted, frozen (−180 °C, liquid nitrogen), and lyophilized. Yield: 5.04 g (84%).

Surface Hydrolysis. Microspheres (1.00 g), ethylene glycol (50 mL), and KOH (2.80 g) were transferred into a 100-mL round-bottom flask.[20] The flask was immersed in an oil bath (180 °C), and the reaction was allowed to proceed for 5 min. Two identical batches were prepared, and these were reacted for 15 and 30 min, respectively. The flask was removed from the oil bath and allowed to cool to room temperature. Microspheres were decanted, washed (water, ethanol, and water, vide supra), frozen, and lyophilized.

Titration of Carboxylic Groups on Microspheres. Microspheres (100 mg) were resuspended in 100 μL of 0.100 M NaOH and 10 μL of phenophthalein (400 mg in 40 mL of 96% ethanol). Carefully small amounts of 0.010 M HCl were added until the color changed from bright purple to colorless.[21] Untreated spheres that do not contain carboxylic groups needed the same amount of HCl to neutralize the solution without spheres. The hydrolyzed spheres were neutralized with less HCl. The difference in added volume of HCl is a direct measure for the amount of carboxylic groups generated on the spheres by surface hydrolysis.

Cytocompatibility of Microspheres. Mouse fibroblasts (3T3 cells) were grown in DMEM/F12 medium containing Glutamax and supplemented with 10% fetal bovine serum and antibiotics (10 U/mL penicillin, 10 μg/mL streptomycin, 0.25 μg/mL amphotericin B). Cells were harvested with 0.05% Trypsin/0.53 mM EDTA and seeded in a 24 well plate at a density of 25 000 cells per well. The cells were allowed to attach for 16 h at 37 °C/5%CO_2. Micropsheres were added in such an amount that approximately 20% of the surface was covered by microspheres. The cells were allowed to grow for a further 48 h, and subsequently photographs were taken with a Leica DM-IL inverted microscope equipped with a Sony DSC-70 digital camera. To quantify cell viability, after the 48 h incubation, medium was exchanged for medium containing 0.5 mg/mL MTT. The cells were incubated for a further 1.5 h at 37 °C. MTT is converted into an insoluble blue/purple formazan by intact mitochondria, meaning incubation with nonviable cells will not result in staining. The medium was aspirated, the formazan was dissolved in 2-propanol, and absorbance at 550 nm was determined as a direct measure for viability.

Surface Coupling of Coumarin. Surface-hydrolyzed microspheres (100 mg) were transferred to a 1-mL Eppendorf tube and washed with MES buffer for 30 min.[22] Then, the supernatant was removed. A stock solution of reactants was prepared as follows: 1-ethyl-3-(3-dimethyl-aminopropyl)carbodiimide (EDC) (191.5 mg, 0.999 mmol), *N*-hydroxy-succinimide (NHS) (46.5 mg, 0.404 mmol), and 7-amino-4-methyl-coumarin (5.0 mg, 0.029 mmol) were dissolved in 5 mL of MES buffer. Then, 1 mL of the stock solution was mixed with the washed microspheres, and the reaction was allowed to proceed for 2 h. The tube was mounted on a carousel that rotated at a slow speed. After 2 h, the supernatant was removed, the microspheres were washed with MES buffer and examined by fluorescence microscopy. The reaction was run for different batches of KOH-treated microspheres (5, 15 or 30 min treated) and for microspheres that did not receive KOH treatment (control).

Protein Immobilization. KOH-treated microspheres (100 mg) were transferred to a 1-mL Eppendorf tube and washed with MES buffer for 30 min.[23] The supernatant was removed. A new stock solution was made, as follows: EDC (191.5 mg, 0.999 mmol) and NHS (46.5 mg, 0.404 mmol) were dissolved in 5.0 mL of MES buffer. Then, 0.5 mL of the stock solution and 0.5 mL of MES buffer were added to the washed microspheres. The Eppendorf tube was mounted on the carousel and rotated for 30 min. The supernatant was discarded, and the microspheres were briefly washed with MES buffer. As proteins, we used (i) porcine alkaline phosphatase (2 mg/mL in MES buffer) and (ii) heat-denatured FITC-labeled bovine collagen I (0.8 mg/mL) in carbonate buffer. In each case, microspheres pretreated with EDC and NHS were incubated with 1 mL of the protein solution for 2 h, while

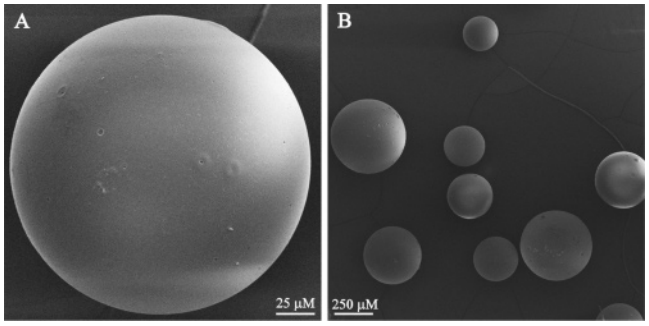

Figure 1. Scanning electron micrographs showing the radio-opaque microspheres at two different magnifications (see bars).

the vial was rotated on the carousel. Subsequently, microspheres were washed repeatedly with MES buffer.

Microspheres, to which alkaline phosphatase was coupled, were incubated with *p*-nitro-phenyl phosphate (PNPP). A solution of PNPP (26.3 mg, 0.1 mmol) and $MgCl_2$ (9.5 mg, 100 μmol) in 10 mL of Tris buffer was made. A total of 1 mL of this solution was added to the microspheres. For all different microspheres, control measurements (microspheres incubated with alkaline phosphatase but without EDC and NHS) were performed, to subtract the contribution of nonspecifically adsorbed alkaline phosphatase. Aliquots were taken regularly, and extinction at 405 nm was determined. Increase in extinction at 405 nm in time is a direct measure for the amount of converted PNPP and thus of the amount of alkaline phosphatase. By comparing conversion rates of the microspheres with the rates of known amounts of alkaline phosphatase, the amount of covalently bound alkaline phosphatase could be estimated.

Collagen-FITC-labeled microspheres were examined directly by fluorescence microscopy. Part of the microspheres was treated with collagenase (0.5 mg/mL) in 10 mM phosphate buffered saline. Fluorescence (ex 485 nm/em 520 nm) was determined with a Gemini XS fluorometer.

X-ray Visibility. X-ray contrast of the microspheres was assessed under routine hospital conditions, using a digital mammography imaging system (ThermoTrex Corporation, San Diego, CA).

Results and Discussion

Microspheres. Iodine-containing radio-opaque cross-linked polymer microspheres readily formed within 3 h during suspension polymerization of the mixture MMA + **1** + TEGDMA. The yield was 84% after workup and lyophilization. The beads were washed thoroughly, to remove traces of unreacted monomers, which would otherwise exert a cytotoxic effect on contacting cells. SEM analysis revealed that the beads are smooth, perfectly spherical, and nonporous (Figure 1).

Of a typical batch, the average diameter was 333 μm, with a standard deviation of 112 μm. Size and size distribution were reproducible, although the exact stirring parameters (speed, depth of the rotating paddle, and flask geometry) influenced the outcome substantially.

As the first step toward functionalization of the microspheres, carboxylic acid groups were generated at the surface, via treatment with KOH in ethylene glycol at 180 °C.[20] The reaction conditions represent a delicate balance: saponification proceeds very slowly at lower temperatures, and higher temperatures or longer reaction times were found to result in structural deterioration of the particles. The reaction was run in three different batches, one for 5 min, one for 15 min, and one for 30 min. We anticipated that a longer reaction time would result in an increased surface density of COOH groups. After treatment, the microspheres were washed thoroughly, to remove the last traces of ethylene glycol. Inadequate washing resulted in coalescence of the particles during lyophilization and loss of the spherical shape. Figure 2 shows SEM micrographs of microspheres after KOH treatment and workup. The smooth surface was preserved in the 5-min treatment (A), whereas the 15-min treatment led to some surface spots (B). After 30 min of KOH treatment (C), the surface became rough with incrustations and some flakes.

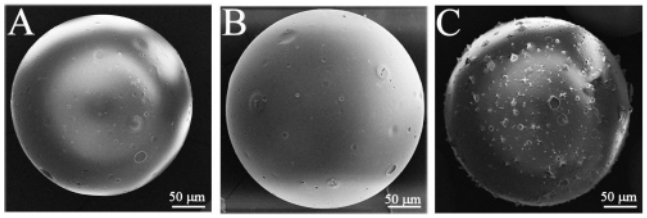

Figure 2. Scanning electron micrograph showing the effect of the incubation with KOH (180 °C) on the surface of the microspheres. (A) 5 min; (B) 15 min; (C) 30 min.

Table 1. Quantitation of COOH Groups on the Surface of Hydrolyzed Microspheres[a]

time of KOH treatment (min)	−COOH groups (μmol/gr spheres)
0	0
5	0.96 ± 0.27
15	1.61 ± 0.41
30	10.26 ± 1.80

[a] The results are the mean of four measurements ±standard deviation.

Quantitative analysis of the COOH groups on the surface was performed by titration, using phenolphthalein as the indicator.[21] The results given in Table 1 demonstrate that with increasing time of KOH treatment an increasing amount of carboxylic groups were generated on the surface of the microspheres. The large increase of carboxylic groups between 15 and 30 min may indicate that the surface of the microspheres starts disintegrating, as can also be seen in Figure 2C.

The presence of COOH groups was also confirmed using a fluorescent chromophore. The dye 7-amino-4-methylcoumarin was coupled to the COOH through an activated ester (NHS) + EDC protocol. This one-step procedure was straightforward; 2 h reaction time was sufficient for clear labeling. Figure 3 shows fluorescence micrographs for the untreated control (A), and KOH-reaction times of 5, 15, and 30 min, respectively (B−D). Differences in fluorescence intensity due to the labeling (A vs B−D), and due to the density of COOH groups at the surface (within the series B − D), are clearly visible.

X-ray Visibility. A model setup was used to test whether our particles feature an adequate level of X-ray visibility. First, we dispersed microspheres from four different batches (untreated and treated with KOH for 5, 15, or 30 min) in molten gelatine, which served to mimic the filler agent. After cooling, the samples were implanted in the soft tissue part of a chicken leg; the bones served as a qualitative internal standard for the X-ray contrast of the particles.[18d] Figure 4 shows the X-ray image. The particles are clearly visible, especially in the expansion (B). It is noteworthy that not only the conglomerated particles are seen; some of the larger particles can also be discerned individually. The images do not reveal any effect of the KOH treatment on the X-ray contrast. This is expected, since the saponification only affects the surface of the particles. We believe, based on Figure 4, and based on comments of an

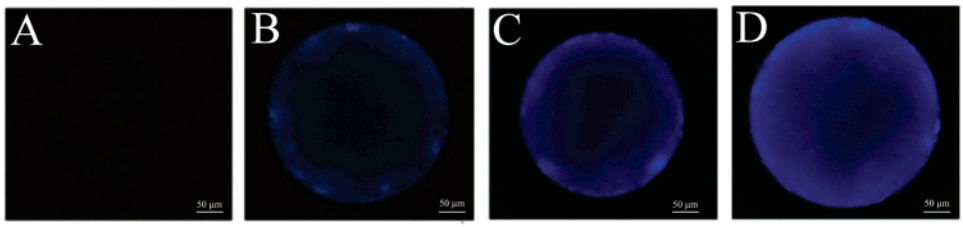

Figure 3. Fluorescence micrographs revealing the presence of immobilized coumarin. (B) Typical microsphere incubated with KOH for 5 min (180 °C), prior to reaction with coumarin; (C) idem, but incubated with KOH for 15 min; (D) idem, but incubated with KOH for 30 min. (A) control; that is, this particle was not treated with KOH, but treated with NHS, EDC and coumarin in an identical manner, as for B−D.

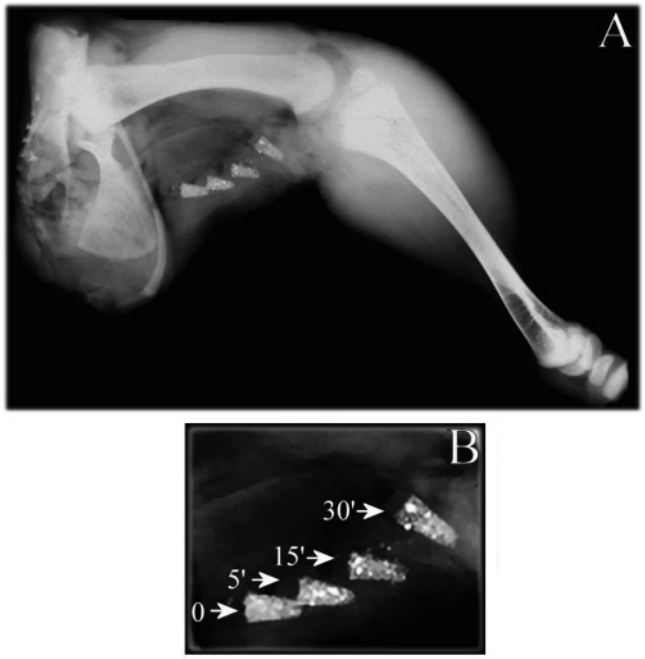

Figure 4. (A) X-ray of the chicken leg with four different samples of the radio-opaque microparticles, embedded in gelatin as a mimic for the filler agent used clinically, implanted in the soft tissue part (see text). (B) Expansion of the soft-tissue containing the four samples.

experienced radiologist, that the particles exhibit sufficient X-ray visibility for clinical use; that is, most likely they would be traceable if injected in peri-urethral tissue to treat SUI in human patients.

Cytocompatibility in Vitro. Growth of cells (mouse 3T3 fibroblasts) in direct contact with our particles was examined in vitro. Figure 5 shows light micrographs, taken after 4 days of incubation. Figure 5A−D reveals that the fibroblasts cells grow readily in the presence of the untreated microspheres (A) and in the presence of KOH-treated microspheres (B−D). Note that cells lie adjacent to the biomaterial's surface in all four cases, which indicates that their affinities for the iodine-containing biomaterial and for the tissue-culture poly(styrene) (TCPS) of the culture plate are comparable. Apparently, the presence of COOH groups does not affect cytocompatibility of the surfaces. Figure 5, panels E and F, represents controls: panel E shows the fibroblasts cultured on TCPS in the absence of any biomaterial, and panel F shows the effect of a toxic biomaterial (latex): much fewer cells are found near the material's surface, and the morphology of the cells is clearly distorted. Cell viability of the cells was determined using a MTT assay in order to quantitatively confirm these results. Figure 5G clearly demonstrates that the microspheres are completely nontoxic.

Immobilization of Proteins. Our first attempt to couple a protein to the surface COOH groups on the microspheres was

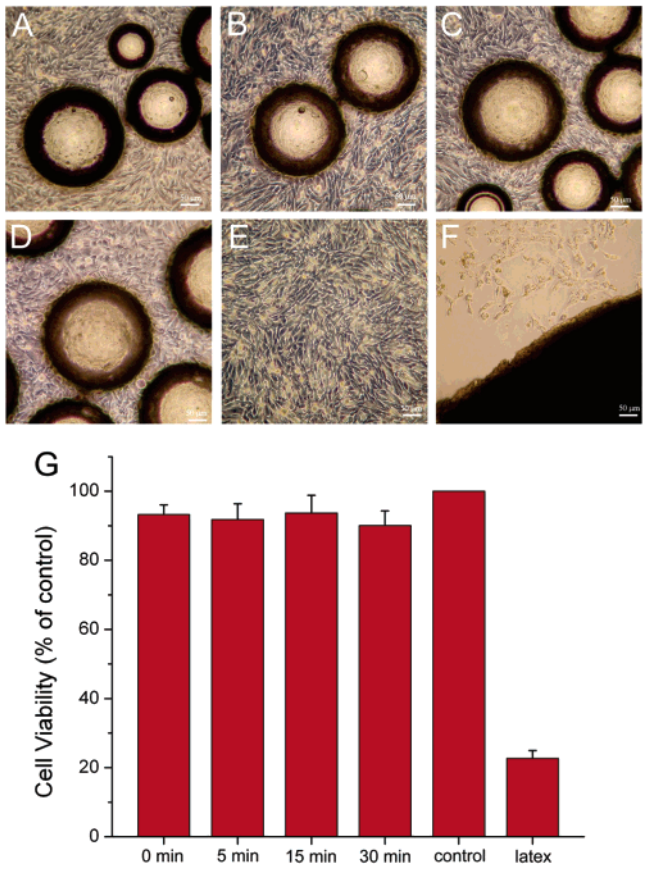

Figure 5. Light microscopic images, taken during the direct-contact cytocompatibility assay. The images were recorded after 4 days of incubation with mouse 3T3 fibroblast cells. (A) Fibroblasts in contact with microspheres that were not incubated with KOH (control); (B) fibroblasts in contact with microspheres that were incubated with KOH for 5 min; (C) idem, but KOH treatment lasted 15 min; (D) idem, but KOH treatment lasted 30 min; (E) fibroblasts proliferating in the absence of any biomaterial (control); (F) 3T3 cells in the presence of Latex, which is a toxic control biomaterial (control).

performed with the enzyme alkaline phosphatase (porcine). An activated ester (NHS)/carbodiimide (EDC) protocol was used, exactly in the same manner as for the coupling of 7-amino-4-methylcoumarin. Spheres were thoroughly washed after the reaction, to remove adsorbed, uncoupled enzyme as much as possible. Incubation of the modified spheres with *p*-nitrophenyl phosphate led to conversion; formation of *p*-nitrophenol could be monitored spectrophotometrically. The occurrence of the reaction implies that the spheres have active enzyme molecules on their surface. Figure 6 shows the increase of the optical density as a function of time, for the microspheres that received 5, 15, or 30 min KOH treatment prior to the reaction with alkaline phosphatase. The data indicate that prolonged KOH treatment first resulted in higher COOH surface density and

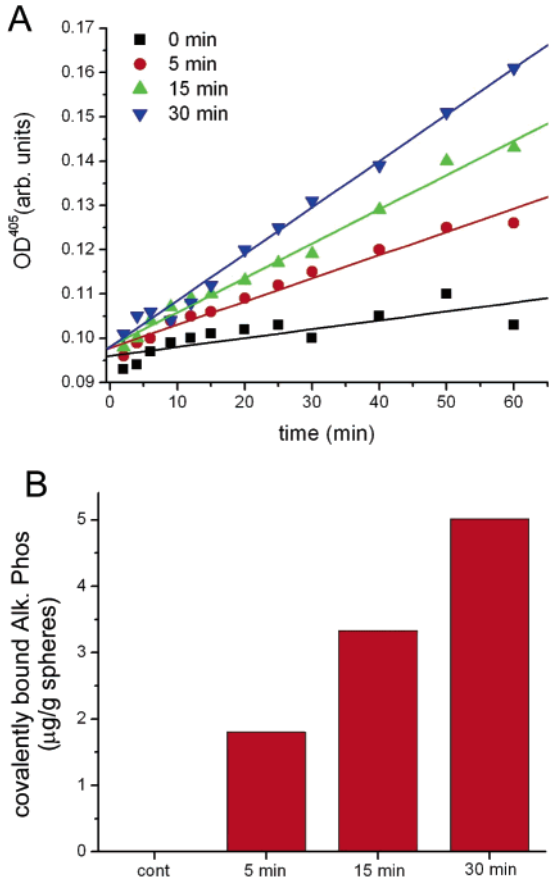

Figure 6. (A) *para*-Nitrophenol formation over time followed by absorbance at 405 nm, in the presence of the different spheres with surface coupled alkaline phosphatase. Note that the rate of the reaction (i.e., the surface density of the enzyme molecules) correlates with the duration of KOH treatment. (B) Amount of covalently coupled alkaline phosphatase to the different spheres, determined by comparing rates of *para*-nitrophenol formation with those of a standard curve of alkaline phosphatase. These data are representative for three independent experiments using different batches of spheres.

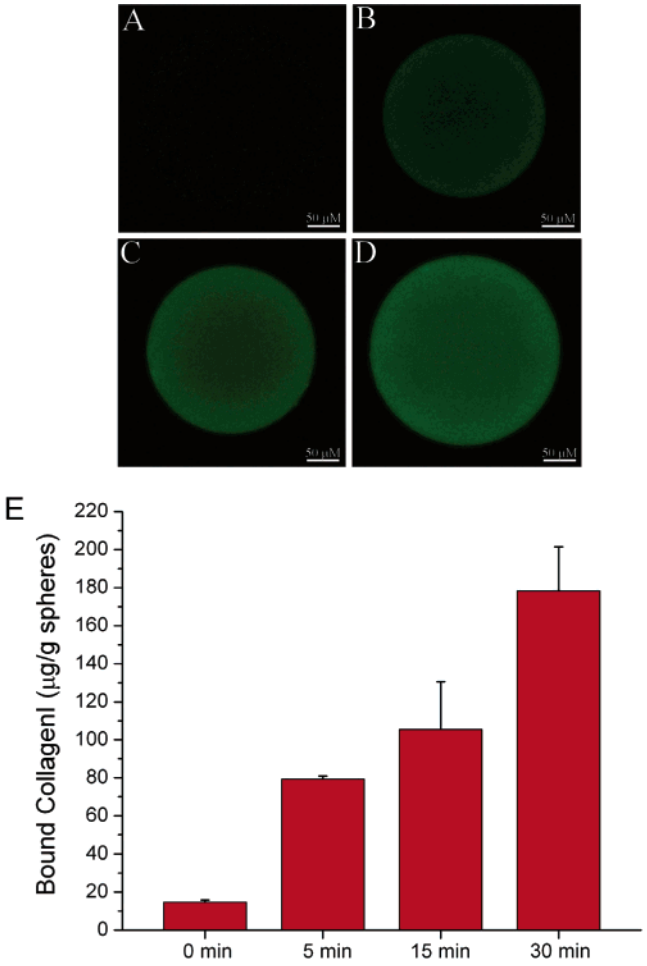

Figure 7. Fluorescence micrographs, showing immobilized fluorescent collagen at the surface of the microspheres (B−D). (B) Microspheres that were incubated with KOH for 5 min prior to reaction with NHS, EDC and labeled collagen; (C) idem, but incubation with KOH lasted 15 min; (D) idem, but incubation with KOH lasted 30 min. (A) Control; that is, this particle was not treated with KOH, but treated with NHS, EDC and labeled collagen in an identical manner as for B−D.

later in higher surface density of active enzyme (Figure 6B). Microspheres that were not treated with KOH served as a control. Furthermore, all spheres were also treated with alkaline phosphatase but without the cross-linking agents EDC and NHS to correct for nonspecific adsorption of alkaline phosphatase (adsorption controls). Upon incubation with PNPP, all control spheres, both the non-KOH treated spheres as well as the adsorption control, demonstrated virtually the same slight *p*-nitrophenyl phosphate conversion. The total amount of covalently surface-linked alkaline phosphatase increases with longer KOH treatment (Figure 6B). The carbodiimide protocol was also used to bind fluorescently labeled collagen to our particles, as was verified through fluorescence microscopy (Figure 7A−D). Note that the fluorescence intensity again correlates with the time of KOH treatment. To quantify collagen coupling, the microspheres were incubated with collagenase. This rendered the supernatant fluorescent and this fluorescence could be compared to known concentrations of fluorescent collagen (Figure 7E). Up to approximately 190 μg per gram of spheres could be covalently coupled.

The apparent possibility to bind collagen to the surface of the microspheres is of great interest with respect to the aim of this study, to explore new methods to prevent migration of injected microparticles in vivo. There are numerous studies that describe strongly increased cell adhesion on surfaces coated with collagen type I that have been well documented, leading to the frequent use of collagen matrixes for tissue engineering purposes.[24] Our ongoing research is directed toward the question of whether immobilized collagen molecules will bind to extracellular matrix proteins (e.g., collagen) that are present in soft tissues. If such molecular recognition and binding occurs, then it must be expected that the microparticles have a decreased tendency to migrate. We will address this question in a series of in vitro and in vivo model studies.

Concluding Remarks

Injectable synthetic polymer microparticles that are currently used in the clinic (e.g., in cosmetic/reconstructive surgery or to treat SUI) all consist of passive biomaterials. Their primary function inside the body is to fill space. Usually, they are surrounded by a fibrous capsule and there is no interaction whatsoever with surrounding tissues. This study makes clear that polymeric microspheres with several different and potentially useful functionalities can be manufactured. First, radiopacity can be introduced through incorporation of covalently bound iodine in the polymer's structure, without affecting the density of the biomaterial and without compromising the

cytocompatibility of the biomaterial. Clinically, it is important that injected biomaterials can be visualized through X-ray fluoroscopy. Moreover, a method to engineer the surface of the particles is described. Attachment of proteins, especially those that are recognized and bound by the extracellular matrix proteins in soft tissues, may turn out to be an effective strategy to prevent migration of injected microparticles away from the site of injection.

Acknowledgment. Thanks are due to the Deutsche Forschungsgemeinschaft (DFG) that financed this study through the Graduiertenkolleg 1035 "BioInterface − Detektion und Steuerung grenzflächeninduzierter biomolekularer und zellulärer Funktionen" in which the Rheinisch Westfälische Technische Hochschule Aachen, and the Universities of Liège and Maastricht cooperate.

References and Notes

(1) (a) Perenack, J. *J. Oral. Maxillofac. Surg*. **2005**, *63*, 1634−1641. (b) Byrne, P. J.; Hilger, P. A. *Facial Plast. Surg.* **2004**, *20*, 31−38. (c) Wall, S. J.; Adamson, P. A. *Otolaryngol. Clin. North. Am.* **2002**, *35*, 87−102.

(2) (a) Jordan, D. R. *Can. J. Ophthalmol.* **2003**, *38*, 285−288. (b) Sclafani, A. P.; Romo, T., III. *Facial Plast. Surg.* **2000**, *16*, 29−34.

(3) (a) Homicz, M. R.; Watson, D. *Facial Plast. Surg.* **2004**, *20*, 21−29. (b) Carruthers, A.; Carruthers, J. D. *Dermatol. Surg.* **2005**, *31*, 1561−1564. (c) Haneke, E. *Semin. Cutan. Med. Surg.* **2004**, *23*, 227−232. (d) Lemperle, G.; Romano, J. J.; Busso, M. *Dermatol. Surg.* **2003**, *29*, 573−587.

(4) (a) ter Meulen, H.; van Kerrebroeck, E. *Expert Rev. Med. Devices* **2004**, *1*, 205−213. (b) Lightner, D. J.; Itano, N. B.; Sweat, S. D.; Chrouser, K. L.; Fick, F. *Curr. Urol. Rep.* **2002**, *3*, 408−413. (c) Lightner, D. J. *Curr. Opin. Urol.* **2002**, *12*, 333−338. (d) Hershorn, S. *Can. J. Urol.* **2006**, *13*, 5−12.

(5) (a) Requena, C.; Izquierdo, M. J.; Navarro, M.; Martinez, A.; Vilata, J. J.; Botella, R.; Amorrortu, J.; Sabater, V.; Aliaga, A.; Requena, L. *Am. J. Dermatopathol.* **2001**, *23*, 197−202. (b) Lemperle, G.; Morhenn, V.; Charrier, U. *Aesthetic Plast. Surg.* **2003**, *27*, 354−366. (c) Christensen, L.; Breiting, V.; Janssen, M.; Vuust, J.; Hogdall, E. *Aesthetic. Plast. Surg.* **2005**, *29*, 34−48. (d) Rubin, J. P.; Yaremchuk, M. J. *Plast. Reconstr. Surg.* **1997**, *100*, 1336−1353.

(6) (a) Lemperle, G.; Morhenn, V. B.; Pestonjamasp, V.; Gallo, R. L. *Plast. Reconstr. Surg.* **2004**, *113*, 1380−1390. (b) Morhenn, V. B.; Lemperle, G.; Gallo, R. L. *Dermatol. Surg.* **2002**, *28*, 484−90.

(7) Zullo, M. A.; Plotti, F.; Bellati, F.; Muzii, L.; Angioli, R.; Panici, P. B. *J. Urol*. **2005**, *173*, 898−902.

(8) (a) Sheriff, M. K.; Foley, S.; Mcfarlane, J.; Nauth-Misir, R.; Shah, P. *J. Eur. Urol.* **1997**, *32*, 284−288. (b) Guys, J. M.; Breaud, J.; Hery, G.; Camerlo, A.; Le Hors, H.; De Lagausie, P. *J. Urol.* **2006**, *175*, 1106−1110. (c) Halachmi, S.; Farhat, W.; Metcalfe, P.; Bagli, D. J.; McLorie, G. A.; Khy, A. E. *J. Urol.* **2004**, *171*, 1287−1290.

(9) (a) Malizia, A. A., Jr.; Reiman, H. M.; Myers, R. P.; Sande, J. R.; Barham, S. S.; Benson, R. C., Jr.; Dewanjee, M. K.; Utz, W. J. *J. Am. Med. Assoc*. **1984**, *251*, 3277−3281. (b) Claes, H.; Stroobants, D.; van Meerbeek, J.; Verbeken, E.; Knockaert, D.; Baert, L. *J. Urol*. **1989**, *142*, 821−822. (c) Kiilholma, P. J.; Chancellor, M. B.; Makinen, J.; Hirsch, I. H.; Klemi, P. J. *Neurourol. Urodyn*. **1993**, *12*, 131−137.

(10) (a) Madjar, S.; Covington-Nichols, C.; Secrest, ChL. *J. Urol.* **2003**, *170*, 2327−2329. (b) Lightner, D.; Calvosa, C.; Andersen, R.; Klimberg, I.; Brito, C. G.; Snyder, J.; Gleason, D.; Killion, D.; Macdonald, J.; Khan, A. U.; Diokno, A.; Sirls, L. T.; Saltzstein, D. *Urology* **2001**, *58*, 12−15.

(11) Pannek, J.; Brands, F. H.; Senge, T. *J. Urol.* **2001**, *166*, 1350−1353.

(12) (a) Bent, A. E.; Foote, J.; Siegel, S.; Faerber, G.; Chao, R.; GormLey, E. A. *J. Urol.* **2001**, *166*, 1354−1357. (b) Corcos, J.; Fournier, C. *Urology* **1999**, *54*, 815−818. (c) Monga, A. K.; Robinson, D.; Stanton, S. L. *Br. J. Urol*. **1995**, *76*, 156−160.

(13) (a) Mayer, R.; Lightfoot, M.; Jung, I. *Urology* **2001**, *57*, 434−438. (b) Bos, S. D.; Ypma, A. F.; Timmermans, C. J. *Br. J. Urol.* **1995**, *76*, 275−276.

(14) (a) Stenberg, A. M.; Larsson, G.; Johnson, P. *Int. Urogynecol. J. Pelvic Floor Dysfunct.* **2003**, *14*, 335−338. (b) van Kerrebroeck, P.; ter Meulen, F.; Larsson, G.; Farrelly, E.; Edwall, L.; Fianu-Jonasson, A. *Urology* **2004**, *64*, 276−281.

(15) (a) Palma, P. C.; Riccetto, C. L.; Herrmann, V.; Netto, N. R. Jr. *J. Endourol.* **1997**, *11*, 67−70. (b) Kanchwala, S. K.; Holloway, L.; Bucky, L. P. *Ann. Plast. Surg.* **2005**, *55*, 30−35.

(16) (a) Sweat, S. D.; Lightner, D. J. *J. Urol*. **1999**, *161*, 93−96. (b) Currie, I.; Drutz, H. P.; Deck, J.; Oxorn, D. *Int. Urogynecol. J. Pelvic Floor Dysfunct.* **1997**, *8*, 377−380. (c) Thaunat, O.; Thaler, F.; Loirat, P.; Decroix, J. P.; Boulin, A. *Plast. Reconstr. Surg.* **2004**, *113*, 2235−2236.

(17) (a) McLennan, M. T.; Bent, A. E. *Obstet. Gynecol*. **1998**, *92*, 650−652. (b) Echols, K. T.; Chesson, R. R.; Breaux, E. F.; Shobeiri, S. A. *Int. Urogynecol. J. Pelvic Floor Dysfunct.* **2002**, *13*, 52−54.

(18) (a) Boelen, E. J.; van Hooy-Corstjens, C. S. J.; Bulstra, S. K.; van Ooij, A.; van Rhijn, L. W.; Koole, L. H. *Biomaterials* **2005**, *26*, 6674−6683. (b) van Hooy-Corstjens, C. S. J.; Aldenhoff, Y. B. J.; Knetsch, M. L. W.; Govaert, L. E.; Arin, E.; Erli, H.; Koole, L. H. *J. Mater. Chem*. **2004**, *14*, 3008−3013. (c) van Hooy-Corstjens, C. S. J.; Govaert, L. E.; Spoelstra, A. B.; Bulstra, S. K.; Wetzels, G. M.; Koole, L. H. *Biomaterials* **2004**, *25*, 2657−2667. (d) Saralidze, K.; Aldenhoff, Y. B. J.; Knetsch, M. L. W.; Koole, L. H. *Biomacromolecules* **2003**, *4*, 793−798. (e) Aldenhoff, Y. B. J.; Kruft, M. A.; Pijpers, A. P.; van der Veen, F. H.; Bulstra, S. K.; Kuijer, R.; Koole, L. H. *Biomaterials* **2002**, *23*, 881−886. (f) Benzina, A.; Kruft, M. A.; van der Veen, F. H.; Bar, F. H.; Blezer, R.; Lindhout, T.; Koole, L. H. *J. Biomed. Mater. Res.* **1996**, *32*, 459−466.

(19) Sivakumar, M.; Panduranga Rao, K. *J. Appl. Pol. Sci*. **2002**, *83*, 3045−3054.

(20) Jayakrishnan, A.; Chitambara Thanoo, B.; Rathinam, K.; Ravi Mandalam, K.; Rao, V. R. K.; Lal, A. V.; Mohanty, M. *Bull. Mater. Sci.* **1989**, *12*, 17−25.

(21) Lewandowski, K.; Svec, F.; Fréchet, J. M. *J. Chem. Mater*. **1998**, *10*, 385−391.

(22) Buttafoco, L.; Engbers-Buijtenhuijs, P.; Poot, A. A.; Dijkstra, P. J.; Daamen, W. F.; van Kuppevelt, T. H.; Vermes, I.; Feijen, J. *J. Biomed. Mater. Res. B Appl. Biomater*. Dec 16, **2005** [Epub ahead of print].

(23) Puleo, D. A.; Kissling, R. A.; Sheu, M. S. *Biomaterials* **2002**, *23*, 2079−2087.

(24) (a) Dewez, J. L.; Lhoest, J. B.; Detrait, E.; Berger, V.; Dupont-Gillain, C. C.; Vincent, L. M.; Schneider, Y. J.; Bertrand, P.; Rouxhet, P. G. *Biomaterials* **1998**, *19*, 1441−1445. (b) McCarthy, J. B.; Vachhani, B.; Lida, J. *Biopolymers* **1996**, *40*, 371−381. (c) Garcia, A. J.; Reyes, C. D. *J. Dent. Res.* **2005**, *84*, 407−413.

BM0603903